THE STRUCTURAL DESIGN OF TALL AND SPECIAL BUILDINGS
Struct. Design Tall Spec. Build. **15**, 3–20 (2006)
Published online in Wiley InterScience (www.interscience.wiley.com). **DOI**: 10.1002/tal.340

NEAR-REAL-TIME LOSS ESTIMATION FOR INSTRUMENTED BUILDINGS

KEITH PORTER*, JUDITH MITRANI-REISER AND JAMES L. BECK
California Institute of Technology, Pasadena, California, USA

SUMMARY

A technique is developed to model instrumented buildings with a second-generation performance-based earthquake engineering approach, producing a damage and loss estimate shortly after the cessation of strong motion. It estimates the likely locations of damage (including concealed structural damage), potentially saving the owner time and money by focusing post-earthquake safety and repair inspections. It provides a rapid estimate of repair costs, allowing the owner quickly to apply for recovery funds or an insurance claim. The method uses basement accelerograms, a stochastic structural model, and nonlinear time-history structural analysis to estimate probabilistic engineering demands (structural response). Structural response is input to fragility functions for each damageable assembly to estimate probabilistic physical damage on a component-by-component basis. Probabilistic repair costs for each assembly are calculated and summed, and contractor overhead and profit are added to produce a probability distribution of total repair cost. A simple Bayesian-updating technique employs upper-story accelerograms to refine the stochastic structural model. It is found in application that using the upper-story accelerograms produces only a modest change in the distributions of damage and repair cost, because most of the uncertainty in repair cost results from the uncertainty in the fragility functions and cost distributions, not from uncertainty in the structural model. Copyright © 2006 John Wiley & Sons, Ltd.

1. INTRODUCTION

The research presented here addresses the question of how sensor data from an instrumented building can inform an analytical model of the building to produce a rapid, post-earthquake estimate of the probabilistic seismic performance of the building. Two general lines of research are relevant here: structural health monitoring (SHM) and loss estimation (LE), which are now merging somewhat with performance-based earthquake engineering (PBEE). Structural health monitoring seeks to establish some knowledge of the current condition of a structure based on data from sensors located on the structure. Loss estimation (and now PBEE) generally seeks to characterize seismic performance of building, bridges, and other facilities in terms of repair costs, human safety, and post-earthquake operability (‘dollars, deaths, and downtime’), typically in the context of an individual facility or a general class of facilities subjected to seismic excitation at some unknown future date.

Sensor information until recently has played little role in LE and PBEE. Celebi *et al.* (2004) recently combined sensor information with PBEE, illustrating their methodology with a 24-story steel-frame building that has been instrumented to compute interstory drift ratios at a few story levels where sensors operate at two adjacent floors. These interstory drift ratios are then compared with (deterministic) drift limits associated with each of several FEMA 273-style performance levels: operational,

*Correspondence to: Keith Porter, California Institute of Technology, 1200 E California Blvd MC 104-44, Pasadena, CA 91125-4400, USA. E-mail: keith@cohen-porter.net

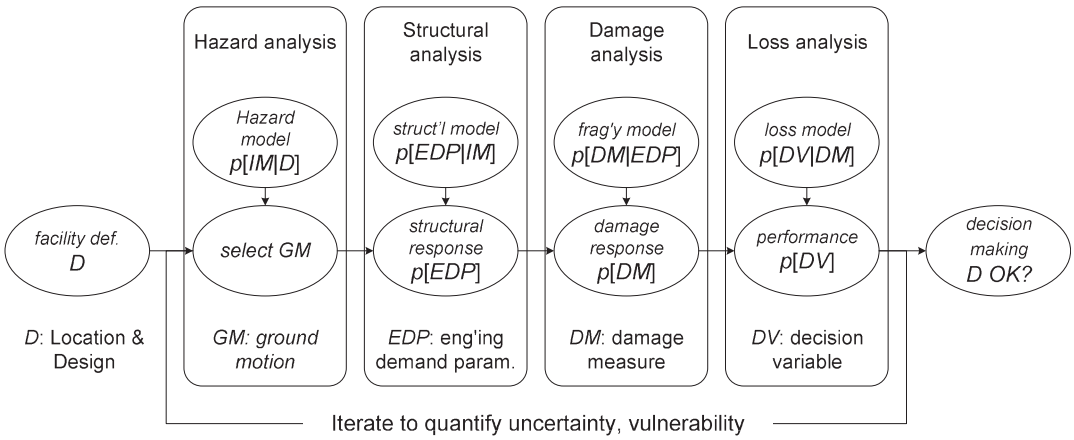

Figure 1. Framework of probabilistic PBEE methodologies

immediately occupiable, life-safety, and collapse-prevention (FEMA, 1997). When a drift limit is exceeded, the associated performance level is assumed to be exceeded.

In the present paper, which summarizes Porter *et al.* (2004), a new approach using more recent PBEE developments is taken, whereby structural response is calculated based on measured basement motion and a stochastic structural model. Bayesian updating is then applied using the upper-story motions to improve the structural model, and fragility functions are employed to predict damage based on the updated model of structural response. This has an advantage that structural responses other than accelerations and interstory drift can be used in the analysis, and both structural and non-structural damage can be addressed using prior information about the fragility of these components. This new approach is detailed later.

Several authors have formulated analytical methods to relate shaking and seismic performance on a building-specific basis. Czarnecki (1973) was perhaps the first to suggest a method that relied on linear structural analysis to estimate structural response, and on simple relationships between structural response and loss to calculate repair cost. Kustu *et al.* (1982) advanced this approach using laboratory and other empirical data to calculate probabilistic damage, and construction-cost information to estimate loss based on damage. In the HAZUS-MH software, Kircher *et al.* (1997) use a similar approach, but using the capacity spectrum method to calculate structural response. Kadakal *et al.* (2000) present a similar approach, using three-dimensional pushover structural analysis. In Beck *et al.* (1999), Porter (2000), Porter and Kiremidjian (2001), and subsequent work, we use stochastic modeling at each analytical stage, nonlinear time-history structural analysis, a more detailed taxonomy of components and new fragility functions, to demonstrate how one can calculate repair costs, repair duration and post-earthquake usability.

These methods generally share four analytical stages, illustrated in Figure 1. The first is a hazard analysis, in which ground-motion time histories are scaled to one or more levels of shaking intensity of interest, parameterized through some intensity measure (IM) such as spectral acceleration. In the second stage, a structural analysis is performed to calculate structural response, parameterized via various engineering demand parameters (EDP), at a component-by-component level. In the third stage, called the damage analysis, EDPs are applied to component fragility functions to estimate physical damage measures (DM) for each component. Finally, a loss analysis is performed using the component DMs. In the loss analysis, various decision variables (DV) are calculated, such as repair cost, casualties, and loss-of-use duration (dollars, deaths, and downtime).

DOI: 10.1002/tal

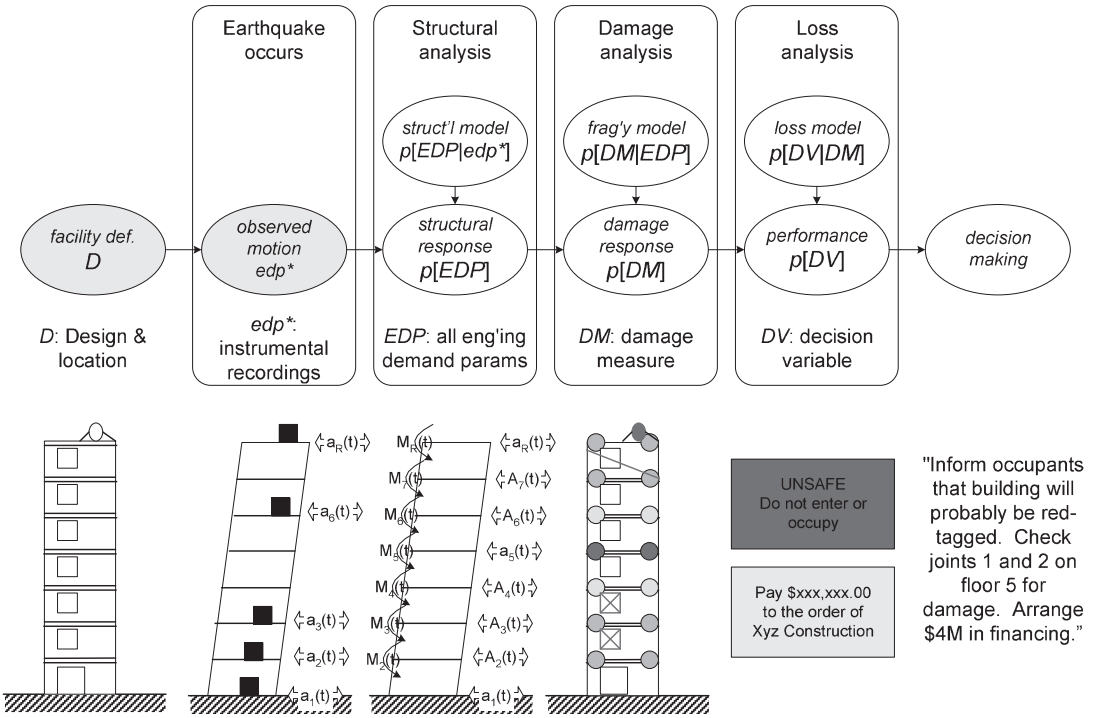

Figure 2. Overview of real-time loss estimation methodology employed here

PBEE researchers have propagated uncertainty in various ways, such as Monte Carlo simulation, Latin Hypercube simulation, and quadrature. Incremental dynamic analysis (IDA) represents MCS applied during the hazard and structural analysis. A first-order, second-moment (FOSM) approximation can be used to reduce the computational effort of the damage and loss analysis, although it appears generally to be the structural analysis that is the computationally costly part of PBEE when nonlinear time-history structural analysis is employed.

2. REAL-TIME PBEE METHODOLOGY

In the present context, the hazard analysis portion of Figure 1 is unnecessary, as the actual base ground-motion time-history is known. Some but not all of the EDPs are also known through sensors at upper stories. The methodology employed here, illustrated in Figure 2, is closely related to Figure 1, with modifications to account for the sensor information. It is now described.

2.1 Facility definition

The facility is defined by its structural and architectural design, and if possible by the mechanical, electrical, and plumbing (MEP) components, as well as the approximate number of occupants. Structural drawings are used to create a nominal structural model (a stochastic structural model will be created from this later). The structural, architectural, and MEP designs are used to create an inventory of damageable components. This inventory is a table that lists damageable components by EDP and provides the quantity of each. For example, one record in the table records the square footage of

DOI: 10.1002/tal

gypsum wallboard partition of a particular category that is subject to peak transient drift at story X along column line Y.

2.1.1 Component categories

The taxonomy by which components are categorized is fairly fine, since small details make big differences in component fragility. For example, in tests of various stud wall systems, Pardoen *et al.* (2000) show that different combinations of sheathing, framing, and connectors can make an order-of-magnitude difference in the drift at which damage occurs. Consequently, to lump all drift-sensitive components together, or simply to lump all stud-wall systems together, introduces unnecessary uncertainty to loss analysis and precludes making design or mitigation decisions based on the differences in performance of competing systems.

2.1.2 EDPs

For structural components, various measures of member force or deformation are of interest, such as peak curvature in reinforced concrete beams and columns; the related Park-Ang damage index; or peak bending moment in brittle steel moment connections. EDPs relevant to nonstructural components typically include peak transient interstory drift at each story and column line and peak horizontal accelerations at each floor. For some purposes, such as modeling jammed doors, it may be useful to capture peak residual drift by story and column line.

2.2 Structural analysis

Nonlinear time-history structural analysis is used here. Input base motion is taken from basement accelerations recorded during the earthquake. To account for uncertainties in the structural analysis, a stochastic structural model is created from the nominal one. A number (S) of simulations or realizations of the stochastic structural model are created, and the input base motion is applied to each, to produce S realizations of estimated EDP.

In creating the stochastic structural model, various model parameters can be taken as uncertain. In the present study, five parameters were treated as uncertain: damping (denoted here by ζ), structural-component initial stiffnesses (denoted generically by K_0), post-yield stiffnesses (denoted by K_1), soil spring stiffnesses (denoted by K_S), and structural strengths (denoted generically by F). In Beck *et al.* (2002), we also included uncertainty in mass, but subsequently found in Porter *et al.* (2002) that uncertainty in mass has minimal impact on uncertainty in repair-cost performance. To create a stochastic structural model, each parameter in the nominal structural model is multiplied by an uncertainty term ε. A vector of such uncertainty terms is given by

$$\boldsymbol{\varepsilon}_X = [\varepsilon_\zeta, \varepsilon_{K0}, \varepsilon_{K1}, \varepsilon_{KS}, \varepsilon_F]^T \tag{1}$$

We create S realizations of the stochastic structural model. For each realization, the nominal structural parameters are multiplied by the appropriate component in the realization of $\boldsymbol{\varepsilon}_X$. Each term in $\boldsymbol{\varepsilon}_X$ is taken as independent and log-normally distributed with a mean value of 1·0 and a coefficient of variation denoted by δ. We have taken the COV of pre- and post-yield stiffness, $\delta_{K0} = \delta_{K1} = 0{\cdot}05$. As in Beck *et al.* (2002), we estimate uncertainty in viscous damping as $\delta_\zeta = 0{\cdot}4$, and uncertainty in strength as $\delta_F = 0{\cdot}11$. Jones *et al.* (2002) review experimental data by others, and report that the COV of soil shear modulus reduction ratio, $G/G_{\max}$, varies with shearing strain, γ; with values as low as 0·15 at $\gamma = 0{\cdot}0001\%$, to nearly 1·0 at $\gamma = 1\%$. We use the value at $\gamma = 0{\cdot}03\%$, $G/G_{\max} = 0{\cdot}35$, as a conservative estimate of δ_{KS}.

DOI: 10.1002/tal

To employ these data in a given simulation $s = 0, 1, \ldots S-1$, one simulates each element j of ε_X as

$$\varepsilon_{X,s,j} = \exp(\Phi^{-1}(u)\beta_j + \ln\hat{\varepsilon}_j) \tag{2}$$

where

$$u = \frac{u_1 + u_2}{S} \tag{3}$$

$$\beta_j = \sqrt{\ln(1+\delta_j^2)} \tag{4}$$

$$\hat{\varepsilon}_j = 1/\sqrt{1+\delta_j^2} \tag{5}$$

in which u_1 is sampled from $\{0, 1, \ldots S-1\}$ with equal probability and without replacement, and $u_2 \sim U(0,1)$. In Equation (2), β_j denotes the logarithmic standard deviation of the model parameter j and $\hat{\varepsilon}_j$ denotes the median value of ε_j. Throughout, the values of u_1 and u_2 are sampled independently for each simulation of each uncertain variable. (This Latin Hypercube sampling approach assures that the tails of each distribution are explored as well as the body).

One could treat the parameters of each particular structural member as independent of the corresponding parameters of other members, but this would tend to underestimate uncertainty by overlooking correlation. We chose to treat parameters of each structural member as perfectly correlated with the corresponding parameter of other structural members. This may overestimate uncertainty in EDP, although earlier research (Porter *et al.*, 2002) suggests that uncertainty in EDP has a minor effect on overall performance uncertainty. This was further supported in the present study.

We developed two methods of updating the probability distribution of structural response to account for observed upper-story motions. The first is a particle filter, capable of employing all of the data in the upper-story acceleration time histories, not just peak values. It was found that the particle filter was impractical to implement in the nonlinear time-history structural analysis, as it required the ability to update the structural model at each time step within a structural analysis model that could handle the material and geometric nonlinearities. A method that used a linear structural analysis was created in Matlab to implement and exercise the filter; see Porter *et al.* (2004, Appendix A) for details. Instead, the following simplified approach was used to perform Bayesian updating of the structural response using a structural model that allowed for geometric and material nonlinearities.

In the simpler approach, one sacrifices the ability to use all the accelerogram data and to update the structural model at each time step. One creates a large number of equiprobable samples of the stochastic structural model, accounting for important uncertainties in the structural model, as noted above. For each realization of the structural model, one performs a complete nonlinear time-history structural analysis, using the observed base excitation as the ground-motion input. One extracts from the calculated structural response the complete *EDP* vector for each sample, as well as the estimated and observed peak displacements at the location of each sensor above the base. One then calculates the posterior probability (or weight) of each model based on observed absolute displacements. These weights will later be used to calculate the probability distribution of damage and loss. The algorithm is as follows.

(1) Get observed base excitation, denoted by u_k, and observed response (relative displacement) at instrument channel locations, denoted by o. Let o_{jk} denote observed relative displacement at channel j, time step k. Let o_j denote the peak relative displacement at channel j (max over k).
(2) Generate S structural realizations ('models') m_s: $s = 0, 1, S-1$, i.e., where s indexes the structural model simulation number, and where each realization has equal (prior) probability $P[m_s] = 1/S$.

DOI: 10.1002/tal

(3) Perform structural analyses using base excitation $u(t)$ and produce estimates of relative displacement at instrument locations $\hat{o}_{sjk}$, where s indexes structural model realization, j indexes instrument channel and k indexes time step.
(4) Extract time-max $\hat{o}_{sj} = \max_k[\hat{o}_{sjk}]$.
(5) Assume modeling error of estimated observation $\hat{o}_j$ has a constant logarithmic standard deviation denoted by β_j. That is, given a deterministic model of the structure and ground motion, we define error ε as $\varepsilon_j = (\ln \hat{o}_j - \ln o_j)$ and take ε_j as normally distributed with mean $E[\varepsilon_j] = 0$ and standard deviation $\beta_j = (\mathrm{Var}[\varepsilon])^{1/2} = 0{\cdot}15$, for all j.
(6) Update weights of each model m_s:

$$w_s = P[m_s|o] = \frac{p[o|m_s]P[m_s]}{\sum_{s=0}^{S-1} p[o|m_s]P[m_s]} \tag{6}$$

where

$$P[m_s|o] = \text{posterior probability of models } s \text{ conditioned on } o$$

$$P[m_s] = \text{prior probability of model } m_s = 1/S$$

$$p[o|m_s] = \text{likelihood of observation } o = \Pi_j[\phi(z_{sj})]$$

$$\phi = \text{Gaussian probability density function}$$

$$z_{sj} = \ln(o_j/\hat{o}_{sj})/\beta_j$$

2.3 Damage analysis

In the damage analysis, one calculates damage to each damageable assembly for each sample *EDP* vector, via assembly fragility functions. Damage and loss are simulated T times for each of N *EDP* vectors. Each damage simulation proceeds as follows.

It is assumed that after an assembly is subjected to a certain *EDP*, it will be in an uncertain damage state *DM*, indexed by $dm = 0, 1, 2, \ldots N_{DM}$, where $dm = 0$ indicates the undamaged state. We assume that the damage states can be sorted in increasing order, either because an assembly in damage state $dm = i + 1$ must have passed through damage state i already, or because the effort to restore an assembly from damage state $dm = i + 1$ necessarily restores it from damage state $dm = i$.

The probability that an assembly will reach or exceed damage state $DM \geq dm$, given that it experiences some excitation $EDP = x$, can be thought of as the cumulative distribution function (*CDF*) of the uncertain capacity of the component. It is referred to as the component fragility function, commonly taken as log-normal:

$$\begin{aligned} F_{dm}(x) &= P[DM \geq dm|EDP = x] \\ &= \Phi\left(\frac{\ln(x/x_m)}{\beta}\right) \end{aligned} \tag{7}$$

where Φ indicates the cumulative standard Gaussian distribution, x_m denotes the median value of the distribution, and β denotes the logarithmic standard deviation of the distribution. For a component with some integer N_{DM} damage states, the cumulative probability distribution of the damage state *DM* is given by

DOI: 10.1002/tal

$$\begin{aligned} F_{DM|EDP=x}(dm) &\equiv P[DM \le dm | EDP = x] \\ &= 1 - F_{dm+1}(x) \qquad 0 \le dm < N_{DM} \\ &= 1 \qquad dm = N_{DM} \end{aligned} \tag{8}$$

where $F_{DM|EDP=x}(dm)$ denotes the cumulative probability distribution of damage state DM evaluated at dm, given that $EDP = x$. One can simulate the damage to each assembly by inverting Equation (8) at a random probability level u, given by

$$dm = F^{-1}_{DM|EDP=x}(u) \tag{9}$$

where $u \sim$ U(0, 1). The simulated damage state of each assembly is then recorded in the vector DM, whose elements are the value of damage measure of each assembly. Note that one could perhaps improve convergence by using Latin Hypercube simulation of damage.

2.4 Loss analysis: repair cost

In the damage analysis, for each of S simulations of EDP, T simulations of damage are created. In the loss analysis for cost, we simulate repair cost once for each simulation of damage. One simulation of repair cost proceeds as follows.

Each assembly type and damage state is associated with one or more possible repair measures, each with an uncertain repair cost. Let $C_{j,dm}$ denote the uncertain cost to restore an assembly of type j from damage state dm; it can be calculated by standard cost-estimation principles. Let $F_{C,j,dm}(c)$ denote its cumulative distribution function evaluated at c. We take these as log-normally distributed with median values x_m and logarithmic standard deviations β specified for each assembly type and damage state. To simulate $C_{j,dm}$, evaluate

$$C_{j,dm} = \exp(\Phi^{-1}(u_1)\beta + \ln x_m) \tag{10}$$

where u_1 is a sample of a uniformly distributed random variable bounded by 0 and 1. Summing over all assembly types and damage states gives the total direct cost to the contractor. The contractor's overhead and profit, denoted here by C_{OP}, is uncertain at the time of the analysis. Supposing that it is uniformly distributed between a and b (with b potentially as high as 50% in catastrophes, but the range more commonly on the order of 15% and 20%), and letting u_2 denote a sample of a uniformly distributed random variable between 0 and 1,

$$C_{OP} = a + (b - a) \cdot u_2 \tag{11}$$

Thus, in a given simulation of loss, the total repair cost, denoted here by RC, is given by

$$RC = (1 + C_{OP}) \sum_{j=1}^{N_j} \sum_{dm=1}^{N_{DM}} N_{j,dm} C_{j,dm} \tag{12}$$

where $N_{j,dm}$ is the number of assemblies of type j in damage state dm, determined in the damage analysis.

This completes one simulation of loss. We have drawn S samples of EDP, each with updated probability w_s, calculated in Equation (6). For each of these, we drew T equiprobable samples of damage

DOI: 10.1002/tal

Table 1. System performance levels (after ASCE, 2000)

L	Performance level	Max. structural perf. level	Max. nonstructural perf. level
1	Operational	*S*-1	*N-A*
2	Immediate occupancy	*S*-1	*N-B*
3	Life safe	*S*-3	*N-C*
4	Collapse prevention	*S*-5	*N-D*

Note: *S-1, S-3, N-A, N-B*, etc., are labels denoting various structural and nonstructural performance levels.

and loss. The cumulative distribution function for the total repair cost RC is calculated from the $S \times T$ simulations of loss by

$$F_{RC}(rc) = P[RC \le rc] = \frac{1}{T}\sum_{s=0}^{S-1}\sum_{t=0}^{T-1} w_s H(rc - RC_{s,t}) \tag{13}$$

where $H = 1$ if the value in parentheses is greater than or equal to 0; $H = 0$ otherwise.

2.5 *Estimate of post-earthquake performance*

To measure the qualitative performance of a building after an earthquake, we use an enhanced version of the building performance levels that are in Vision 2000 (SEAOC, 1996), FEMA 273 (FEMA, 1997), and FEMA 356 (ASCE, 2000). The structural performance levels of FEMA 356 are collapse prevention, life safety, and immediate occupancy, denoted by *S*-5, *S*-3, and *S*-1, respectively. The descriptions of structural damage associated with each performance level are fairly detailed, addressing damage to different structural components such as primary concrete frames, and describing the degree of damage to individual components and how widespread that level of damage may be, but the descriptions of extent are qualitative, using terms such as 'few', 'distributed' and 'many'. The interested reader is referred to ASCE (2000, Table C1–3) for a list of structural components and descriptions of their damage by performance level.

The nonstructural performance levels of FEMA 356 are similarly detailed, describing degree and extent of damage to a wide variety of nonstructural components, such as cladding. There are four nonstructural performance levels, *N-A* (operational) to *N-D* (hazards reduced), from best to worst. FEMA 356 contains tables that define these performance levels, listing the degree and extent of damage by system and performance level; they are omitted here for brevity. There is also an overall facility performance level, (indexed here by *L*) defined in terms of both structural and nonstructural performance levels, as shown in Table 1. See ASCE (2000, Table C1–5) for nonstructural components and descriptions of their damage by performance level.

While the authors of FEMA 356 caution that the list of structural and nonstructural component performance descriptions are incomplete and should not be used as criteria for determining overall facility performance, the lists nonetheless represent convenient quantitative benchmarks of performance, once the qualitative terms ('few', 'distributed', etc.) are quantified. The present study employed fuzzy sets to quantify these terms. The translation is shown in Table 2 and Figure 3, using a damage fraction, denoted here by *DF*, defined as the fraction of components in the noted damage state.

The FEMA 356 authors describe damage not in terms of repairs required (as we have done), but somewhat more qualitatively, e.g., 'minor spalling'. In Table 2, we have done our best to map our

DOI: 10.1002/tal

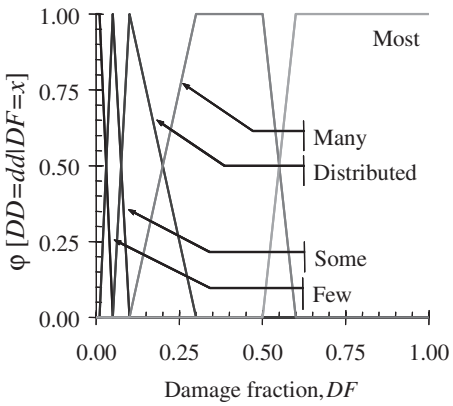

Figure 3. Membership functions relating damage description to damage fraction

Table 2. Translations of qualitative performance terminology

D	Damage description	Damage fraction	Example
1	Negligible, few, little	0–5%	'Generally negligible [ceiling] damage': between 0 and 5% of ceiling area is damaged
2	Some, minor, limited	1–10%	'Some cracked [glazing] panes; none broken': Between 1% and 10% of lites visibly cracked; no glass fallout
3	Distributed	5–30%	'Distributed [partition] damage': between 5% and 30% of partitions need patching, painting or repair, measured by lineal feet
4	Many, extensive	10–60%	'Many fractures at [steel moment frame] connections': between 10% and 60% of connections suffer rejectable damage
5	Most	50–100%	'Most [HVAC equipment] units do not operate': at least 50% of HVAC components inoperative

damage descriptions to theirs, and feel that the mapping is reasonable. We therefore offer our procedure as at least illustrative of what can be done.

Let D denote the damage description of a particular structural or nonstructural component. Under a reasonable reading of ASCE (2000), there are five distinct qualitative damage descriptions, as listed in Table 2. Let d denote a particular value of D. Figure 3 illustrates how these translations lead to membership functions for each damage description.

For example, if 20% of partitions are damaged in a given simulation, one enters Figure 3 with $DF = 20\%$, and observes that the degree of membership that the partition damage can be considered to be 'distributed' is 50%, and a 50% degree of membership that one would consider that 'many' partitions are damaged, i.e., $\varphi[D = 3 \mid DF = 0{\cdot}20] = \varphi\,[D = 4 \mid DF = 0{\cdot}20] = 0{\cdot}5$. From fuzzy-set theory, the membership function $\varphi[D = d \mid DF = df]$ is to be interpreted as a measure of the degree to which one feels that the damage description d is appropriate for a subsystem if its damage factor $DF = df$. For notational convenience, let

$$\varphi_d(df) = \varphi[D = d|DF = df] \tag{14}$$

DOI: 10.1002/tal

and

$$\Phi_d(df) = \varphi[D \le d | DF = df] \tag{15}$$

which gives the degree to which one feels that the appropriate damage description for the component is at most d when the fraction of elements in the component that are in a prescribed damage state is df. From fuzzy set theory

$$\Phi_d(df) = \max\{\varphi_d(df), \varphi_{d-1}(df), \ldots, \varphi_1(df)\} \tag{16}$$

Henceforth, we drop the damage fraction df from the notation for Φ, leaving it implicit. Now, in each of $S \times T$ simulations of structural response and damage, and for each component, we have one value of Φ_d giving the degree to which the component can be said to have damage description no greater than d.

From ASCE (2000), for each component and performance level, we have a particular value of the damage description. For example, for primary concrete frames at structural performance level $S - 1$ (part of the operational facility performance level, $L = 1$, as shown in Table 1), one expects minor hairline cracking and limited yielding at a few locations, i.e., damage description 2. In the present approach, these values are treated as maximum criteria, and denoted by Δ.[1] That is, if for every component and performance level l, if $d \le \Delta(l)$, then the facility is in that performance level or better.

Recall that we are dealing with fuzzy-set descriptions of damage, so we speak in terms of the degree to which each component can be said to have damage description d. Since the fuzzy set corresponding to the performance level is the intersection of the fuzzy sets corresponding to each criterion that must be satisfied, we take the minimum of the membership values for each criterion. Let $\varphi(l)$ denote the membership of the facility in performance level $L = l$, i.e., the degree to which the facility can be described as being in performance level l. Then

$$\varphi(l) = \min(\Phi_\Delta) \tag{17}$$

where the minimum is taken over all structural and nonstructural components.

The membership function in Equation (17) can be thought of as a probability that the facility is in performance level l, given a particular simulation of the structural model and damage state of each component. Considering all $S \times T$ simulations, the probability that the facility satisfies performance level l is estimated by the appropriate weighted average of $\varphi(l)$ based on the usual Monte Carlo method:

$$P[L = l] = \frac{1}{T} \sum_{s=0}^{S-1} \sum_{t=0}^{T-1} w_s \varphi_{st}(l) \tag{18}$$

where w_s is given by Equation (6), and the value of $\varphi(l)$ is calculated for each s and t.

3. SAMPLE APPLICATION

3.1 *Facility definition*

The sample facility is a real, seven-story, 66 000 square-foot hotel located in Van Nuys, CA. It was built in 1966 according to the 1964 Los Angeles City Building Code. The building was lightly damaged

[1]Again, this was not the intent of the authors of ASCE (2000), but it does nonetheless provide a convenient means to quantify performance level in simple terms with some rigor.

DOI: 10.1002/tal

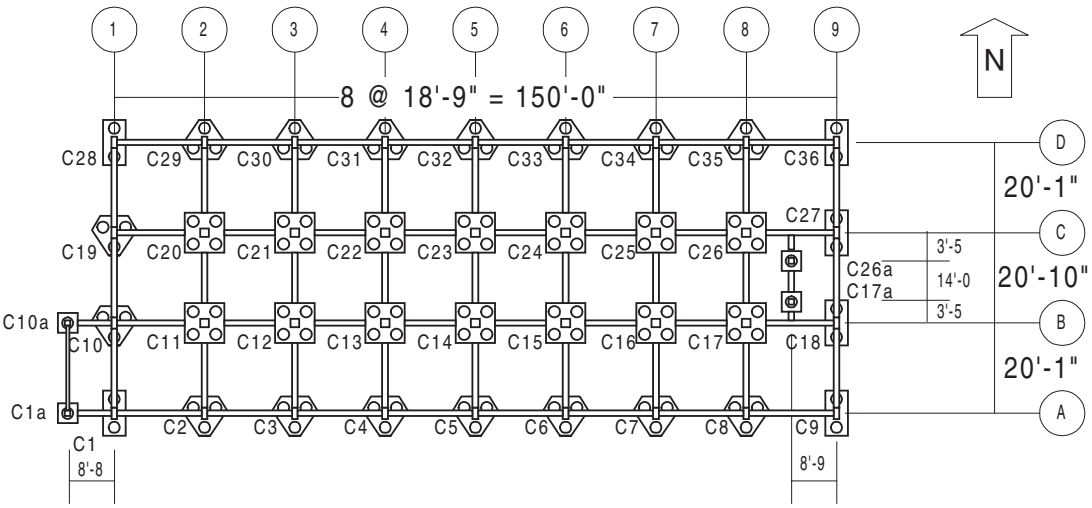

Figure 4. Foundation and column plan, showing designer's notation for column numbers

by the M6.6 1971 San Fernando event, approximately 20 km to the northeast, and severely damaged by the M6.7 1994 Northridge earthquake, whose epicenter was approximately 4·5 km to the southwest. The building has been studied extensively (e.g., Jennings, 1971; Scholl *et al.*, 1982; Islam, 1996a, 1996b; Islam *et al.*, 1998; Li and Jirsa, 1998). Also, Trifunac *et al.* (1999) and Browning *et al.* (2000) provide a detailed account of the physical damage to the structure in the 1994 Northridge earthquake.

In plan, the building is 63 feet by 150 feet, three bays by eight bays, seven stories tall. The long direction is oriented east–west. The building is approximately 65 feet tall, with a tall first story containing a lobby, meeting rooms and various other support services, and upper stories containing hotel suites accessed via a central corridor running along the longitudinal axis of the building. We estimate the replacement cost of the facility to be approximately \$7·0 million, based on square footage and using RS Means Co., Inc. (2001).

The structural system is a cast-in-place reinforced concrete moment-frame building with nonductile column detailing. Perimeter moment frames provide the primary lateral force resistance, although the interior columns and slabs also contribute to lateral stiffness. The gravity system comprises two-way reinforced concrete flat slabs supported by square columns at the interior and the rectangular columns of the perimeter frame. The column plan (with the designer's column numbers) is shown in Figure 4. The building is founded on 24-inch diameter drilled piers in groups of two, three, and four piers per pile cap. Pier lengths vary between 31·5 and 37 feet. Frames are regular in elevation; the south frame elevation is shown in Figure 5. These figures show the designer's notation for beam and column numbering.

Column concrete has nominal strength of $f'_c = 5$ ksi for the first story, 4 ksi for the second story, and 3 ksi from the third to the seventh stories. Beam and slab concrete is nominally $f'_c = 4$ ksi at the second floor and 3 ksi from the third floor to the roof. Column reinforcement steel is A432-62T (Grade 60) for billet bars. Beam and slab reinforcement is ASTM A15-62T and A305-56T (Grade 40) for intermediate grade, deformed billet bars.

DOI: 10.1002/tal

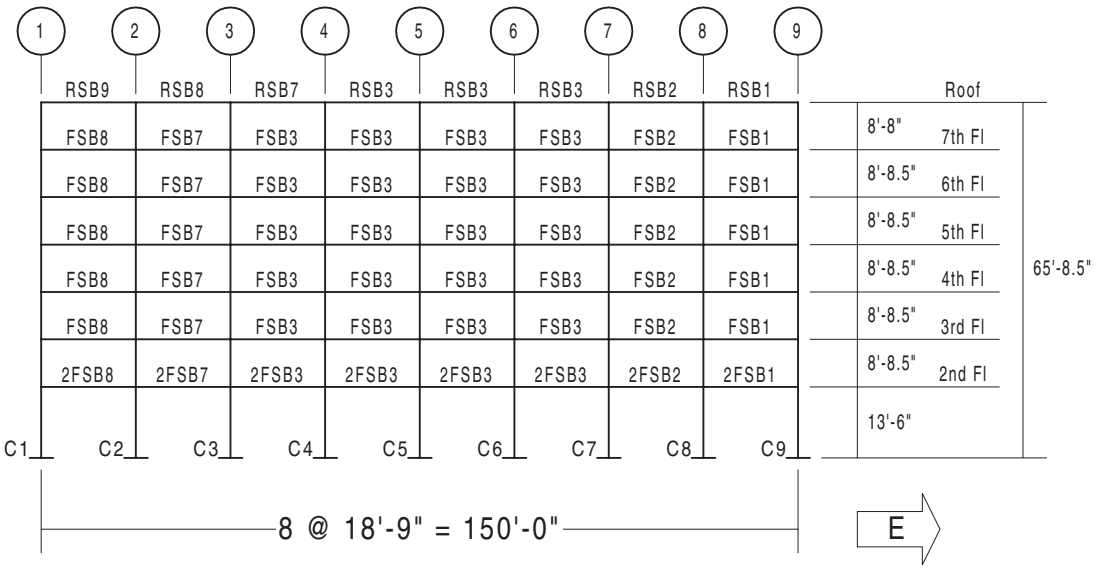

Figure 5. South frame elevation, omitting stair tower at west end

The ground floor has full-height masonry infill walls in the north frame between column lines 5 and 9, and partial-height masonry walls between column lines 1 and 5. Above the second floor there are no other stiff elements between the columns that might produce a short-column effect. The building is clad on the north and south facades with aluminum window walls, comprising $^{3}/_{16}$-inch heavy sheet glass in sliding frames, and $^{1}/_{4}$-inch cement asbestos board panels with an ornamental sight-obscuring mesh of baked enamel or colored vinyl. The east and west end walls are finished on the inside with gypsum wallboard and on the outside with stucco.

Interior partitions are constructed of 5/8-inch gypsum wallboard on $3^{5}/_{8}$-inch metal studs at 16-inch centers. Ceilings in the hotel suites in the second through seventh stories are a textured coating applied to the soffit of the concrete slab above. At the first floor, ceilings are suspended wallboard or acoustical ceiling tiles (2-foot grid). Upper-story hallway ceilings are suspended ceiling on 2×4-foot tee-bar grid, just deep enough to accommodate fluorescent fixtures (approximately 2 inches).

Through-wall air-conditioning units are mounted in the waist panels below the windows and provide ventilation to the suites. Central HVAC is provided only for hallway and ground-floor spaces. Building-service equipment include, on the ground floor: switchgear and transformers (unanchored, unbraced); anchored hot water heater and washing machines; and unanchored dryers and water softener; and on mechanical pads in the parking lot: an unanchored transformer and an anchored diesel backup generator. On the roof, there are two anchored elevator motors, an anchored upright 1000-gallon water tank, anchored cooling tower (for lobby air conditioning) on steel skids, a kitchen fan on possible unanchored 12-inch pipe stilts, and two packaged air-conditioning units on two steel skids each supported by two welded 12-inch pipe stilts that do not appear to be anchored to their base.

3.2 Instrumentation, historic shaking, and damage

In the M6.6 1971 San Fernando event, strong motion instruments recorded peak accelerations at the ground floor of 240 cm/s^2 in the transverse direction, 130 cm/s^2 longitudinally, and 170 cm/s^2 in the

DOI: 10.1002/tal

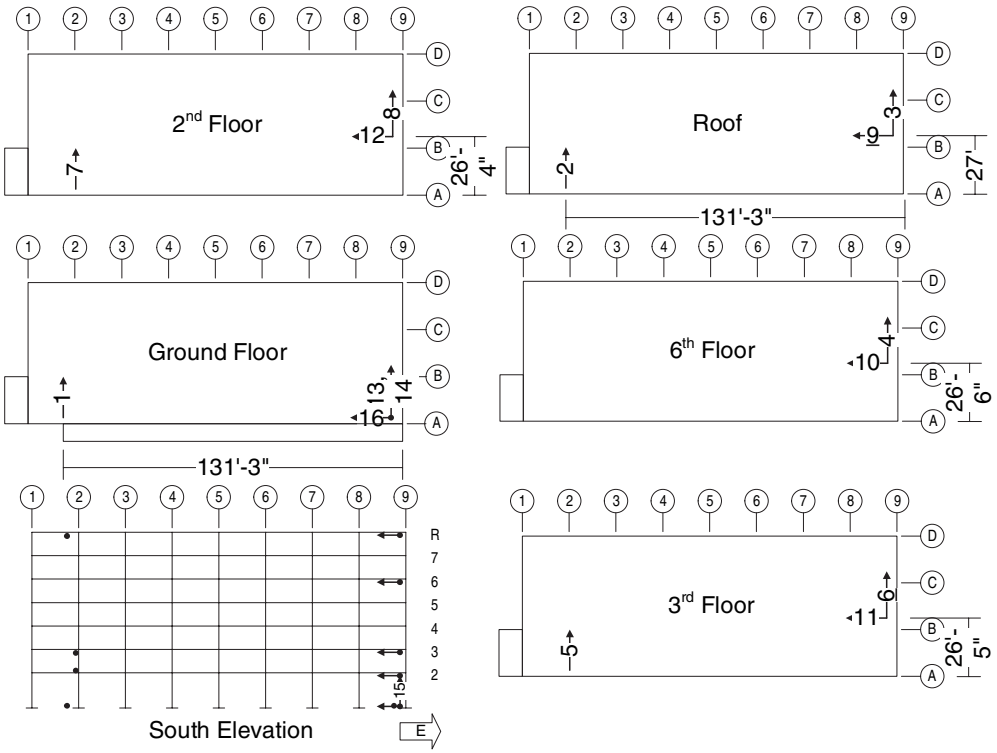

Figure 6. Instrument locations after 1980

vertical direction. Peak roof accelerations were 384 cm/s^2 transverse and 315 cm/s^2 longitudinally at the southwest corner of the building (Trifunac *et al.*, 1999).

The damage in 1971 mostly required architectural repairs. Jennings (1971) describes 'extensive damage to the interior plaster walls, to the plumbing fixtures, etc., on the second, third, and fourth floors. The upper three floors were not damaged severely. . . . The structural frame received some cracks, indicating strains beyond the elastic limit; the cracks were repaired with epoxy cement.' John A. Blume & Associates (1973) provide more detail about the damage, and report the repair cost as 'approximately $145 000', of which $2000 was for structural repair. Trifunac *et al.* (1999) report the cost of repair as $143 000, while Jennings (1971) estimated repair costs as approximately $250 000.

In 1980, additional accelerometers were installed; their locations are shown in Figure 6 (CSMIP, 2001). As of this writing, they have been triggered in 11 subsequent events. According to the available literature, and judging by construction permits on file in the Los Angeles Department of Building and Safety, none of these subsequent events other than the Northridge series caused significant damage.

Shaking, structural response, and damage in the 1994 Northridge earthquake were more severe than in the San Fernando earthquake. Peak acceleration at the ground floor was 440 cm/s^2 in the longitudinal direction and 390 cm/s^2 transversely. Assuming a fundamental period of 1·5–2·0 s and 5% viscous damping, the building experienced damped elastic spectral acceleration of approximately 0·3–0·5 g.

Islam (1996a) reports structural response in the Northridge earthquake in terms of relative displacements and transient interstory drift ratios. Several authors have estimated peak responses at the other floors; Li and Jirsa (1998) and Browning *et al.* (2000) generally agree that transient drift ratios

DOI: 10.1002/tal

reached approximately 2% in the first through fourth stories, decreasing to 0·5% toward the seventh story.

Trifunac *et al.* (1999) and Trifunac and Hao (2001) present damage surveys performed in early 1994. They report extensive structural damage, in the form of shear failure of columns and beam–column joints in the perimeter moment frame. The failures include spalling of the cover concrete over longitudinal bars, buckling of the longitudinal bars and through-cracks up to several inches wide. Damage to the south frame occurred at six locations on the fifth floor and one at the third-floor level. Damage to the north frame occurred in the full-height infill masonry walls at the first story, and at the base of the short columns at the first story in three column lines. Damage to the north frame also occurred at or within the beam–column joint at 12 other locations at the second through fifth floors.

Structural repairs after the 1994 Northridge earthquake involved the addition of shear walls at three columns of the south frame and four columns of the north frame, and at several interior column lines. Base fixity is provided to the new shear walls by the addition of grade beams spanning between pier groups.

3.3 Structural response, damage, and loss

The structural model employed here is an enhancement of the one used in Beck *et al.* (2002), with the addition of soil springs in place of the fixed-based columns assumed in our prior study. As justified in Porter *et al.* (2002), we take mass as deterministic and stiffnesses (initial, post-yield, and soil-spring), damping, and strengths as uncertain. Coefficients of variation for uncertain parameters are as described earlier. Hutchinson (2003) provides a model of soil-spring stiffness for this building. Base excitation u_k is taken from channel 16 as shown in Figure 6. Observed relative displacements o_{jk} are taken from channels 9, 10, 11, and 12 (roof, sixth, third, and second floors, respectively). The values o_j are taken as the peak response over time: $o_j = \max_k(o_{jk})$. Parameters of fragility functions and unit-repair costs used here are tabulated in Porter *et al.* (2004). Contractor overhead and profit is taken as 17·5% of total repair costs to the contractor.

The demonstration building was analyzed using the motion recorded at the base during the 1994 Northridge earthquake. We used $S = 100$ simulations of the structural model and *EDP*. The structural analyses took approximately 4 h on an ordinary desktop computer. Because the subsequent damage, performance, and loss analyses could be performed much more quickly, we used each *EDP* vector $T = 10$ times, thus performing a total of 1000 simulations of structural response, damage, and loss.

Our model predicts extensive damage in third-story columns and roof beams, whereas the actual damage was concentrated at the top of the fourth-story columns and in their joints with fifth-floor beams. None of the predicted most-likely damage locations actually experienced damage in the Northridge earthquake. The implication is that either (a) actual structural conditions in the building differed in some important way from those shown on the construction documents, (b) the fragility functions employed here are incorrect or inappropriate for the beam–columns in the case-study building, or (c) both are true. In any case, since actual damage was due to shear, and since the fragility functions used here are based on flexure, it seems that our fragility functions need reconsideration.

In every simulation, damage to beam and column elements exceeded that allowed under the life-safety performance level. This implies near certainty that the building would not be in the life-safety performance level when exposed to the 1994 Northridge earthquake. Since that is in fact what did happen in Northridge, our model merely implies that, had such a real-time loss estimation system been in place at the time of the 1994 Northridge earthquake, it would have accurately and with near certainty predicted the system performance level.

DOI: 10.1002/tal

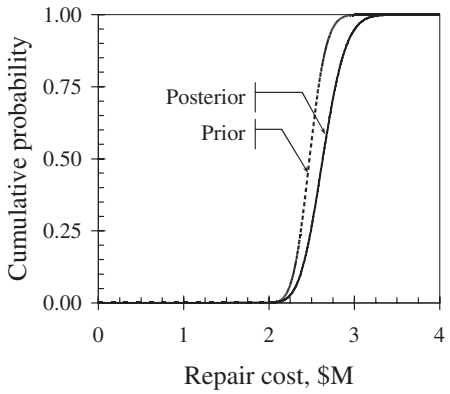

Figure 7. Hindcast repair cost distributions for the 1994 Northridge earthquake

The prior and posterior probability distributions of repair cost are shown in Figure 7. The distributions were almost perfectly log-normally distributed, with median values of $2·5 and $2·6 million, respectively, and logarithmic standard deviations of 0·06 and 0·08, respectively. We have no information about the actual repair cost of the building after the 1994 Northridge earthquake; only that the repairs were costly enough to cause a several-year closure of the building.

Note that reduced uncertainty about damping and stiffness that comes from the earthquake response records does not produce reduced uncertainty regarding *RC*. This observation can perhaps be explained by noting that one expects to reduce uncertainty regarding an uncertain variable *X* when one observes samples of *X*, but not necessarily when one observes samples of another variable *Y* related in some nonlinear fashion to *X*. For example, a more accurate fundamental period can put the structural model closer to a spectral peak in the base motion.

A second, and more important, observation from the similarity of the prior and posterior *RC* distributions is that Bayesian updating of *RC* is almost immaterial, at least in the present case study. That is, observing structural response and comparing it with the calculated value does not add much information at the level of the repair cost. In hindsight, this is a predictable result. We observed in Porter *et al.* (2002) that the greatest contributors to uncertainty in *RC* were the intensity measure (denoted by *IM*, and measured, for example, by damped elastic spectral acceleration), detailed ground-motion time history, denoted by $a(t)$, and assembly capacity, with structural parameters contributing only modestly to uncertainty in *RC*. In the case of real-time loss estimation, *IM* and $a(t)$ are known, and the Bayesian updating using observed EDPs provides no information about assembly capacity, and thus cannot affect the uncertainty associated with it. The minor change in the *RC* distribution observed here is due primarily to reduced uncertainty about damping and stiffness.

We conclude from this observation that perhaps it is not much help to perform Bayesian updating of *EDP* in real-time loss estimation, or even to consider uncertainty in the structural model, when the structural uncertainties seem to contribute so little to overall uncertainty in *RC*. To ignore structural uncertainty would be a valuable timesaver. There would be no need to simulate the structural model and no need to perform numerous nonlinear time-history structural analyses. One need only perform a single deterministic nonlinear time-history structural analysis using the input ground motion recorded at the building base, and then perform the (much faster) damage and loss analyses of ABV as usual. In addition, ignoring structural uncertainties would save time and money in that there would be no need to install instruments on upper floors: structural analysis with a best-estimate structural model appears to provide a good-enough estimate of upper-story response so that the instruments are irrele-

DOI: 10.1002/tal

vant for purposes of real-time loss estimation (but, of course, are of interest for the purpose of investigating the structural properties and response).

4. CONCLUSIONS AND FUTURE DIRECTIONS

4.1 Macroscopic versus component-level accuracy

In this and a Japanese case study not discussed here, we found that hindcasting of the overall system performance was very good, but prediction of detailed damage was poor. We infer that either (a) as-built conditions tend to differ substantially from those shown on the structural drawings, (b) inappropriate fragility functions were employed, or (c) both. In both cases the models suggesting likely damage concentrated at one floor while actual damage occurred at another, which might lend weight to hypothesis (a).

4.2 Is a stochastic structural model needed?

In the case study, we used a simplified particle filter to update *EDP* and found that the above-base sensor data add little information to the performance prediction, probably because structural uncertainties are relatively unimportant compared with the uncertainties regarding assembly damageability. The implication is that real-time loss estimation may be insensitive to structural uncertainties and so costly simulations of structural response may be avoided, and real-time loss estimation does not benefit significantly from instruments other than those at the base of the building.

4.3 Opportunities for implementation

Because much of the cost of applying this algorithm results from the cost of instrumentation and the effort of setting up a structural model, the readiest application would be to instrumented buildings whose structural models are already available. Furthermore, the methodology might produce the most value when applied to important facilities such as those required for emergency response, and buildings with high cost of testing for concealed damage, such as steel-frame structures.

ACKNOWLEDGEMENTS

The work was performed in collaboration with M. Miyamura, A. Kusaka, T. Kudo, K. Ikkatai, and Y. Hyodo. It was funded in part by the CUREE–Kajima Joint Research Program Phase V and by the GW Housner Fund. This work was also supported in part by the Earthquake Engineering Research Centers Program of the National Science Foundation, under award number EEC-9701568 through the Pacific Earthquake Engineering Research Center (PEER). Any opinions, findings, and conclusions or recommendations expressed in this material are those of the author(s) and do not necessarily reflect those of the National Science Foundation.

REFERENCES

ASCE (American Society of Civil Engineers). 2000. *FEMA-356: Prestandard and Commentary for the Seismic Rehabilitation of Buildings*. Washington, DC.

Beck JL, Kiremidjian A, Wilkie S, Mason A, Salmon T, Goltz J, Olson R, Workman J, Irfanoglu A, Porter K. 1999. *Decision Support Tools for Earthquake Recovery of Businesses. Final Report: CUREE-Kajima Joint Research Program Phase III*. Consortium of Universities for Earthquake Engineering Research, Richmond, CA.

DOI: 10.1002/tal

Beck JL, Porter KA, Shaikhutdinov KA, Au SK, Mizukoshi K, Miyamura M, Ishida H, Moroi T, Tsukada Y, Masuda M. 2002. *Impact of Seismic Risk on Lifetime Property Values: Final Report*. Consortium of Universities for Research in Earthquake Engineering, Richmond, CA, http://resolver.caltech.edu/caltechEERL:2002.EERL-2002-04 [18 January 2006].

Browning J, Li Y, Lynn A, Moehle, JP. 2000. Performance assessment for a reinforced concrete frame building. *Earthquake Spectra* **16**(3): 541–555.

CSMIP (California Strong Motion Instrumentation Program). 2001. *Van Nuys 7-Story Hotel, CSMIP Station No. 24386.* California Division of Mines and Geology, Sacramento, CA, ftp://ftp.consrv.ca.gov/pub/dmg/csmip/BuildingData/24386_VanNuys_7-story_Hotel/[22 February 2006].

Celebi M, Sanli A, Sinclair M, Gallant S, Radulescuc D. 2004. Real-time seismic monitoring needs of a building owner—and the solution: a cooperative effort. *Earthquake Spectra* **20**(2): 333–346.

Czarnecki RM. 1973. Earthquake damage to tall buildings. *Structures Publication 359*, Massachusetts Institute of Technology, Cambridge, MA.

FEMA (Federal Emergency Management Agency). 1997. *FEMA-273: NEHRP Guidelines for the Seismic Rehabilitation of Buildings*, Washington, DC.

Hutchinson T. 2003. Analytical modeling of foundation. In *PEER Performance-Based Earthquake Engineering Methodology: Structural and Architectural Aspects*, Krawinkler H (ed.). Pacific Earthquake Engineering Research (PEER) Center: Richmond, CA.

Islam MS. 1996a. Analysis of the response of an instrumented 7-story nonductile concrete frame building damaged during the Northridge Earthquake. In *Proceedings of the 1996 Annual Meeting of the Los Angeles Tall Buildings Structural Council*, 10 May 1996, Los Angeles, CA.

Islam MS. 1996b. Holiday Inn. In *1994 Northridge Earthquake Buildings Case Study Project Proposition 122: Product 3.2*. Seismic Safety Commission, Sacramento CA; 189–233.

Islam MS, Gupta M, Kunnath S. 1998. Critical review of the state-of-the-art analytical tools and acceptance criterion in light of observed response of an instrumented nonductile concrete frame building. In *Proceedings, Sixth US National Conference on Earthquake Engineering*, Seattle, WA, 31 May–4 June 1998. Earthquake Engineering Research Institute, Oakland, CA.

Jennings PC. 1971. Engineering features of the San Fernando Earthquake of February 9, 1971. *Report EERL 71–02*, California Institute of Technology, Pasadena, CA.

John A. Blume & Associates. 1973. Holiday Inn (29). In *San Fernando, California, Earthquake of February 9, 1971*, Vol. 1, Part a. National Oceanographic and Aviation Administration, Washington, DC; 359–393.

Jones AL, Kramer SL, Arduino P. 2002. Estimation of uncertainty in geotechnical properties for performance-based earthquake engineering. *Report PEER 2002/16*, Pacific Earthquake Engineering Research (PEER), Center, Richmond, CA.

Kadakal U, Kishi NG, Song J, Byeon J. 2000. An objective methodology for the assessment of building vulnerability to earthquakes and the development of damage functions. In *Proceedings, Risk 2000 Conference*, Italy.

Kircher CA, Nassar AA, Kustu O, Holmes WT. 1997. Development of building damage functions for earthquake loss estimation. *Earthquake Spectra* **13**(4): 663–682.

Kustu O, Miller DD, Brokken ST. 1982. *Development of Damage Functions for Highrise Building Components*, for the US Department of Energy. URS/John A Blume & Associates, San Francisco, CA.

Li YR, Jirsa JO. 1998. Nonlinear analyses of an instrumented structure damaged in the 1994 Northridge Earthquake. *Earthquake Spectra* **14**(2): 245–264.

Pardoen GC, Kazanjy RP, Freund E, Hamilton CH, Larsen D, Shah N, Smith A. 2000. Results from the city of Los Angeles–UC Irvine shear wall test program. In *Proceedings, 6th World Conference on Timber Engineering*, http://timber.ce.wsu.edu/Resources/papers/1-1-1.pdf [18 January 2006].

Porter KA. 2000. *Assembly-Based Vulnerability of Buildings and its Uses in Seismic Performance Evaluation and Risk-Management Decision-Making*. Doctoral dissertation, Stanford University, Stanford, CA, and ProQuest Co., Ann Arbor, MI, pub. 99–95274, http://wwwlib.umi.com/dissertations/preview/9995274 [18 January 2006].

Porter KA, Kiremidjian AS. 2001. Assembly-based vulnerability and its uses in seismic performance evaluation and risk-management decision-making. *Report No. 139*, John A. Blume Earthquake Engineering Center, Stanford, CA, http://keithp.caltech.edu/publications.htm [18 January 2006].

Porter KA, Beck JL, Shaikhutdinov RV. 2002. Sensitivity of building loss estimates to major uncertain variables. *Earthquake Spectra* **18**(4): 719–743.

Porter KA, Beck JL, Ching JY, Mitrani-Reiser J. 2004. Real-time loss estimation for instrumented buildings. *Report EERL 2004–08*, California Institute of Technology, Pasadena, CA, http://caltecheerl.library.caltech.edu/374 [18 January 2006].

DOI: 10.1002/tal

RS Means Co., Inc. 2001. *Means Square Foot Costs*. Kingston, MA.

Scholl RE, Kustu O, Perry CL, Zanetti JM. 1982. Seismic damage assessment for high-rise buildings. *URS/JAB 8020.* URS/John A. Blume & Associates, San Francisco, CA.

SEAOC (Structural Engineers Association of California). 1996. Vision 2000, conceptual framework for performance-based seismic design. *Recommended Lateral Force Requirements and Commentary, 1996* (6th edn). Sacramento, CA; 391–416.

Trifunac MD, TY Hao. 2001. 7-storey reinforced concrete building in Van Nuys, California: photographs of the damage from the 1994 Northridge Earthquake. *Report CE 01–05*, University of Southern California Department of Civil Engineering, Los Angeles, CA, http://www.usc.edu/dept/civil_eng/Earthquake_eng/CE_Reports/01_05/01_05_ALL.PDF [18 January 2006].

Trifunac MD, Ivanovic SS, Todorovska MI. 1999. Instrumented 7-storey reinforced concrete building in Van Nuys, California: description of the damage from the 1994 Northridge Earthquake and strong motion data. *Report CE 99–02*, University of Southern California Department of Civil Engineering, Los Angeles, CA.

DOI: 10.1002/tal